

**Retro-aldol-type Fragmentation of Reducing Sugars Preferentially
Occurring in Polyether at High Temperature: Role of the Ether
Oxygen as a Base Catalyst**

Seiji Matsuoka, Haruo Kawamoto*, Shiro Saka

* Corresponding author: Haruo Kawamoto

Graduate School of Energy Science, Kyoto University

Yoshida-honmachi, Sakyo-ku, Kyoto 606-8501, Japan

Tel/Fax: +81-75-753-4737

E-mail address: kawamoto@energy.kyoto-u.ac.jp

Abstract:

1 The pyrolysis behavior of reducing monosaccharides was compared in the
2 presence and absence of tetraethyleneglycol dimethylether (TEGDE), a polyether
3 ($N_2/150-250$ °C). The pyrolytic pathways changed drastically in TEGDE. Glucose
4 started to decompose at >160 °C under the neat conditions, and polysaccharides,
5 anhydrosugars (levoglucosan and 1,6-anhydroglucofuranose), a colored substance and
6 char were the major products. However, glucose was completely stabilized against
7 decomposition in TEGDE and instead converted into fragmentation products including
8 formaldehyde, glycolaldehyde, glyceraldehyde, 1,3-dihydroxyacetone, erythrose and
9 erythrulose at higher temperatures. The total yield of the fragmentation products
10 reached a 74.9 wt % at 250 °C. An aldose-ketose isomerization and retro-aldol
11 fragmentation including a six-membered cyclic transition state were suggested as the
12 principle mechanisms. Several other polyethers gave similar results. This unique
13 property of polyether can be explained by the basicity of the ether oxygen which acts as
14 a proton acceptor for the hydroxyl groups in the sugar. This H-bonding between the
15 polyether and glucose may prevent inter- and intramolecular H-bonding (H-donation to
16 the oxygen atoms) of glucose, which results in stabilization against transglycosylation
17 and dehydration reactions. Such inter- and intramolecular H-bonding (H-donation) may
18 also be involved in the thermal decomposition of the melt sugar as an activation (acid
19 catalysis) mechanism.

20

21 **Keywords:**

22 Reducing sugar; Controlled pyrolysis; Polyether; Retro-aldol fragmentation; Hydrogen
23 bond.

24

25 **1. Introduction**

26 Pyrolysis is an effective method for obtaining fuels and chemicals from organic
27 resources. Methanol used to be produced from wood pyrolyzates [1]. Catalytic cracking
28 is currently available for production of gaseous and liquid fuels and commodity
29 chemicals from petroleum [2,3]. Biomass has great potential as a future renewable
30 resource for fuels and chemicals production [1,4]. Thermochemical methods such as
31 fast pyrolysis [5,6] and gasification [5,7] are promising ways for converting biomass
32 into fuels and chemicals. However, low product selectivity arising from the complex
33 reactions of biomass pyrolysis makes the application of these pyrolysis-based processes
34 difficult. Understanding the molecular mechanisms of biomass pyrolysis and their
35 control would be useful for improving the product selectivity.

36 Carbohydrates are a major component of biomass resources, and hence,
37 pyrolysis of reducing [8,9] and non-reducing sugars [10-12] and polysaccharides
38 [13-15] has been studied extensively. Reducing monosaccharides are known to be
39 degraded at a much lower temperature range ($> 160\text{ }^{\circ}\text{C}$) than the non-reducing sugars,
40 and their thermal decomposition has been discussed in connection with a caramelization
41 process [8]. Thermal glycosylation into polysaccharides and formation of furanic
42 compounds, char and colored substances through dehydration are reported to be
43 pyrolytic reactions occurring during caramelization [8]. At temperatures higher than $>$
44 $250\text{ }^{\circ}\text{C}$, formation of low molecular weight (MW) products including anhydrosugars
45 (levoglucosan (1,6-anhydro- β -D-glucopyranose), 1,6-anhydro- β -D-glucofuranose),
46 furanic compounds (furfural, 5-hydroxymethylfurfural), fragmentation products
47 (hydroxyacetone, glycolaldehyde) and organic acids (acetic acid, formic acid, etc.)
48 becomes more important [8,16,17].

49 Recently, Hosoya et al. [18] have reported that levoglucosan, an important
50 intermediate in cellulose pyrolysis, was selectively converted into gaseous products (CO
51 and CO_2) in the gas phase at $400\text{ }^{\circ}\text{C}$, while it was converted into polysaccharides, char

52 and low MW products as described above in the liquid phase. Thus, the pyrolytic
53 pathway varies depending on the phase of pyrolysis, that is, gas or liquid phase. As a
54 related phenomenon, Hosoya et al. [19] also reported that levoglucosan was stabilized
55 up to 350°C in aromatic substances, and they related this unexpected feature to the
56 dispersion of levoglucosan molecules in the aromatic substance through C-H/ π
57 interactions.

58 Because of the drastic differences in the reactivity reported for some pyrolysis
59 conditions, we hypothesize that inter- and intramolecular hydrogen bonding initiates the
60 pyrolysis reactions such as glycosylation and dehydration of sugars. Hydrogen-donation
61 to the oxygen atoms of the sugar may act as an acid catalysis at high temperature. To
62 confirm this hypothesis, polyether, which is expected to act only as a hydrogen acceptor,
63 was tested. Most of the experiments were conducted with tetraethyleneglycol
64 dimethylether (TEGDE) as the model polyether because this has a high boiling point
65 (280 °C) and can solubilize glucose up to 2 wt % (150 °C). Pyrolysis of aldo (glucose
66 and glyceraldehyde) and keto (fructose and 1,3-dihydroxyacetone) sugars was
67 conducted in TEGDE. The roles of intra and intermolecular hydrogen bonding in sugar
68 pyrolysis are discussed.

69

70

71 **2. Experimental**

72 2.1. Materials

73 Glucose, fructose, and glyceraldehyde were from Nacalai Tesque Inc., Japan.
74 Glycolaldehyde, 1,3-dihydroxyacetone, erythrose, and erythrulose were from
75 Sigma-Aldrich Co., USA. Tetraethyleneglycol dimethylether, 18-crown-6, isosorbide
76 dimethylether, diethyleneglycol dibutylether, and levoglucosan were from Tokyo
77 Chemical Industry Co. Ltd., Japan. Cellotriose and cellohexaose were purchased from
78 Seikagaku Biobusiness Corporation, Japan. 1,6-Anhydro- β -D-glucofuranose was

79 prepared by heat treatment of glucose in sulfolane (tetramethylene sulfone) at 250 °C.

80

81 2.2. Method of sugar pyrolysis

82 Sugar (20 mg), polyether (2 g) including 3,5-dibutyl hydroxyl toluene (BHT,
83 0.5 wt % as a stabilizer), and a glass-coated stir bar were placed at the bottom of a 30 mL
84 flask. A condenser, a three-way tap, and a nitrogen balloon were connected to the flask.
85 After the air inside the reactor was replaced with N₂ by using an aspirator connected
86 through the three-way tap, the flask was heated in an oil bath which was preheated at
87 150-250 °C, and the mixture was stirred with a magnetic stirrer for 10-60 min. After
88 heating, the flask was removed from the oil bath and cooled with flowing air (30 s) and
89 then in cold water (30 s). BHT was used as a stabilizer for polyether. However,
90 influences of the addition of BHT on the products composition were only small under
91 the present pyrolysis conditions. Neat sugar pyrolysis was also conducted without
92 addition of polyether, BHT, and the stir bar.

93

94 2.3. Recovery of the products and unreacted sugar

95 To remove polyether and BHT, *n*-hexane (20 mL) was added to the reaction
96 mixture. The mixture was left for 1 h at room temperature to give a colorless crystalline
97 substance or a syrup as the precipitate, which was recovered by centrifugation at 8000
98 rpm for 10 min. After washing with another 20 mL of *n*-hexane and subsequent drying
99 in air, the precipitate was dissolved in 2 mL of water, and 0.1 mL of the resulting
100 solution was dried in a vacuum desiccator and subsequently trimethylsilylated with a
101 0.1 mL of silylation reagent (BSTFA: TMCS: Pyridine = 2:1:7) at 60 °C for 10 min.
102 Recovery of the unreacted sugar was measured by GC-FID analysis. The GC analysis
103 was performed on a Shimadzu GC-14B with the following chromatographic conditions,
104 column: CBP5-M25-O25 (25 m, 0.22 mm in diameter), injector temperature: 250 °C,
105 detector temperature: 250 °C, column temperature: 160→250 °C (0→9 min), 250 °C

106 (9→15 min), carrier gas: He, flow rate: 1.5 mL/min, detector: FID.

107

108 2.4. Isolation and identification of the products

109 The mixtures obtained as the precipitates were purified further using silica gel
110 column chromatography; eluent: chloroform and then 20% MeOH/chloroform.
111 Formaldehyde was recovered according to the method as described below.
112 Glycolaldehyde, glyceraldehyde, 1,3-dihydroxyacetone and erythrose were identified by
113 comparing the ¹H-NMR spectra of these oxime derivatives (with hydroxylamine) with
114 those of the authentic compounds. Chemical shift and coupling constant were shown as
115 δ and Hz, respectively. The ¹H-NMR spectra were measured in D₂O on a Varian
116 AVANCE 400 spectrometer (400MHz): Glycolaldehyde oxime (*Z*, *E*-isomer): δ 7.49 (t,
117 $J = 4.8$, 1 H, H-C=N, *E*), 6.90 (t, $J = 4.0$, 1 H, H-C=N, *Z*), 4.35 (t, $J = 4.0$, 2 H,
118 -CH₂-OD, *Z*), 4.13 (d, $J = 4.8$, 2 H, -CH₂-OD, *E*); 1,3-dihydroxyacetone oxime: δ 4.44
119 (s, 2 H), 4.25 (s, 2 H); glyceraldehyde oxime (*E*-isomer): δ 7.42 (d, $J = 6.0$, 1 H, C₁-H),
120 4.27 (ddd, $J = 4.8, 6.0, 6.0$, 1 H, C₂-H), 3.65 (dd, $J = 4.8, 12.0$, 1 H, C₃-H), 3.61 (dd, $J =$
121 $6.0, 11.6$, 1 H, C₃-H); erythrose oxime (*E*-isomer): δ 7.47 (d, $J = 6.4$, 1 H, C₁-H), 4.18 (t,
122 $J = 6.4$, 1 H, C₂-H), 3.75-3.79 (m, 1 H, C₃-H), 3.67 (dd, $J = 4.0, 12.0$, 1 H, C₄-H), 3.55
123 (dd, $J = 6.4, 12.0$, 1 H, C₄-H). erythrose was identified by comparing the ¹H-NMR
124 spectrum (without oximation) with the authentic compound: δ 4.55 (d, $J = 19.2$, 1 H,
125 C₁-H), 4.48 (d, $J = 19.2$, 1 H, C₁-H), 4.41 (t, $J = 4.0$, 1 H, C₃-H), 3.82 (d, $J = 4.0$, 1 H,
126 C₄-H), 3.81 (d, $J = 4.0$, 1 H, C₄-H).

127

128 2.5. Quantification

129 Quantification of the products was carried out by GC-FID after oxime-TMS
130 derivatization according to the method reported by Hosoya et al. [20] The reaction
131 mixture in the flask and on the condenser wall was carefully extracted with 5 mL of
132 pyridine which included anthracene (10 mg, as an internal standard) and hydroxylamine

133 hydrochloride (50 mg, as an oximation reagent). 0.05 mL of the solution was
134 trimethylsilylated with a 0.1 mL of silylation reagent (BSTFA: TMCS: pyridine = 2:1:7)
135 at 60 °C for 10 min. The GC analysis was performed on a Shimadzu GC-14B with the
136 following chromatographic conditions: column: CBP5-M25-O25 (25 m, 0.22 mm in
137 diameter), injector temperature: 250 °C, detector temperature: 250 °C, column
138 temperature: 120°C (0→1 min), 120→170°C (1→13.5 min), 170→250 °C (13.5→23.5
139 min), 250 °C (23.5→28 min), and carrier gas: He, flow rate: 1.5 mL/min, detector: FID.

140 Quantification of formaldehyde was difficult due to the recovery problem of
141 the gaseous formaldehyde. With a liquid N₂ trap, formation of formaldehyde from
142 glyceraldehyde and 1,3-dihydroxyacetone was confirmed. For quantitative analysis by
143 GC-FID, benzylhydroxylamine hydrochloride (200 mg) was used as an oximation
144 reagent instead of hydroxylamine hydrochloride, and biphenyl (10 mg) was used as an
145 internal standard instead of anthracene. The GC analysis was conducted with a slightly
146 changed column temperature profile: 120 °C (0→3 min), 120→180 °C (3→9 min),
147 180 °C (9→13 min), 180→250 °C (13→16.5 min), 250 °C (16.5→18 min). Since a
148 small amount of formaldehyde was also observed in a blank test (without any sugars)
149 due to thermal decomposition of TEGDE, the formaldehyde yields in this paper are
150 presented after correction for this formaldehyde arising from the TEGDE
151 decomposition.

152

153 2.6. GPC analysis

154 The GPC analysis of the water soluble products was performed on a Shimadzu
155 LC-10 with the following chromatographic conditions: column: Asahipak GS-220,
156 column temperature: 60 °C, eluent: water, flow rate: 0.5 mL/min, detector: RI and UV
157 254nm.

158

159 2.7. FTIR analysis

160 IR Spectra were recorded with a Shimadzu IR-8300 spectrometer using a liquid
161 cell. The mixtures of 1,3-dihydroxyacetone and various amounts of TEGDE were
162 preheated at 150 °C before analysis to solubilize 1,3-dihydroxyacetone completely in
163 TEGDE.

164

165

166 3. Results and discussion

167

168 3.1. Pyrolysis behavior of glucose in the presence or absence of TEGDE

169 Fig. 1 shows the photographs of the pyrolyzates (neat conditions: solubilized in
170 1 mL of water after pyrolysis) (a) and temperature dependency (b) of the recovery of
171 glucose in the presence or absence of TEGDE (N₂/ 30 min). Under neat conditions,
172 color formation was observed at > 160 °C, and the color darkened with increasing
173 temperature. At 240 °C the formation of char, which was not soluble in water, was
174 additionally observed. The decrease in glucose recovery was correlated with the
175 coloration and char formation.

176 Glucose was comparatively stabilized in TEGDE as shown by the higher
177 glucose recovery at each temperature (Fig. 1(b)). Interestingly, even at 250 °C where
178 glucose disappeared completely, the solution after pyrolysis in TEGDE remained almost
179 colorless without formation of any insoluble products (char) (Fig. 1 (a)). Accordingly,
180 formation of char and colored substances was completely inhibited in TEGDE, even
181 though glucose decomposed into other substances.

182 Using GPC, the MW distribution of the pyrolyzates can be determined as
183 illustrated in Fig. 2. Under the neat conditions, the intensity of the glucose signal (18.5
184 min) decreased with increasing temperature, and broad signals in the higher MW region
185 became significant (Fig. 2 (a)). These results indicate that the oligosaccharides
186 formation through thermal glycosylation reaction proceeded under the neat conditions.

187 Similar glycosylation is reported for glucose [21] and the reducing end of cellulose [22].
188 Although no significant signals were observed at 150-200 °C with an UV_{254nm} detector,
189 higher MW products obtained at 220 °C showed obvious UV absorptivity which
190 suggests the conjugated double bond formed through dehydration.

191 The pyrolyzates obtained in TEGDE gave very different chromatograms (Fig. 2
192 (b)). No signals were observed in the higher MW region other than the glucose signal.
193 The decreasing rate of the intensity of the glucose signal with increasing temperature
194 was lower than that of neat glucose pyrolysis. This is consistent with the recovery data
195 (Fig. 1(b)). Instead of the formation of high MW products under the neat condition, the
196 product signals were observed in the lower MW region.

197 Fig. 3 shows the results of GC-FID analysis of the pyrolyzates obtained at
198 220 °C/30 min (as TMS derivatives). Chromatograms (b) and (d) show the results of the
199 oximation products in an effort to identify the low MW hydroxyl aldehydes and
200 hydroxyl ketones. Under the neat conditions (Fig. 3 (a) and (b)), levoglucosan (0.98
201 wt%) and its furanose isomer (0.71 wt%) were identified at 8.2 and 8.6 min,
202 respectively. These are the products of the intramolecular glycosylation of glucose after
203 pyranose-furanose isomerization. These signals were not observed in the pyrolyzates
204 obtained in TEGDE (Fig. 3 (c) and (d)). The lack of formation of these anhydrosugars
205 suggests that the inhibition of the oligosaccharides formation in TEGDE is not
206 explainable merely by the dilution effect. Formation of a reactive intermediate itself
207 would be inhibited in TEGDE, although the glycosylation mechanism is not
208 well-understood. On the contrary, glycolaldehyde, glyceraldehyde,
209 1,3-dihydroxyacetone, erythrose and erythrulose were identified as their oxime-TMS
210 derivatives (*Z* and *E* isomers). Formation of these products was also confirmed by
211 ¹H-NMR analysis of the isolated compounds.

212 Based on these characterization results, it is concluded that glucose is
213 selectively converted into several fragmentation products without undergoing

214 glycosylation and dehydration reactions which give anhydrosugars, oligosaccharides,
215 char and colored substances.

216

217 3.2. Fragmentation pathway in TEGDE

218 To obtain more information on the fragmentation pathway, glyceraldehyde and
219 1,3-dihydroxyacetone were pyrolyzed in TEGDE as the simplest aldo and keto sugars,
220 respectively. Fig. 4 shows the time course of the product formation from these sugars.
221 Gaseous formaldehyde was difficult to analyze. The formaldehyde yields presented here
222 are the tentative values obtained by collection using a liquid N₂ trap. In the early stage
223 of reaction, a significant amount of 1,3-dihydroxyacetone was formed from
224 glyceraldehyde. Thus, the aldose-ketose isomerization (Lobry-de Bruyn-van Ekenstein
225 transformation) is an important initial reaction (Fig. 5). The
226 1,3-dihydroxyacetone/glyceraldehyde ratios were usually much higher than 1 during
227 pyrolysis of these sugars, even glyceraldehyde. This suggests that 1,3-dihydroxyacetone
228 is more favorable in this aldose-ketose isomerization probably due to its greater stability
229 arising from its more substituted carbonyl structure.

230 Glycolaldehyde and formaldehyde were formed from these C3 sugars. This is
231 explained with the retro-aldol-type fragmentation mechanism (Fig. 5). A six-membered
232 cyclic transition state may be involved in this reaction according to the literature
233 reporting the thermal decomposition of β -hydroxy ketones [23] and esters [24].
234 1,3-Dihydroxyacetone, which cannot form such a cyclic transition state, is more stable
235 against fragmentation than glyceraldehyde. Glycolaldehyde and formaldehyde observed
236 during the pyrolysis of 1,3-dihydroxyacetone would be formed via glyceraldehyde after
237 isomerization.

238 Product formation behaviors from C6 sugars, glucose (an aldose) and fructose
239 (a ketose), are shown in Fig. 6. Gaseous formaldehyde was not collected in these
240 experiments. The suggested fragmentation mechanisms starting from their open-chain

241 forms are also illustrated in Fig. 7. Their product compositions were more complicated
242 than those of the C3 sugars, since some C4 sugars, that is, erythrose (an aldose) and
243 erythrulose (a ketose), were additionally observed. These C4 sugars are expected to
244 form by splitting off of the C2 glycolaldehyde from the reducing (reaction c) and
245 non-reducing (reaction i) sides of the sugars.

246 Glucose gave fructose in the early stage of pyrolysis at 220 °C, and the yield
247 reached 7.2 wt% of the amount of the reacted glucose at 10 min. Accordingly,
248 glucose-fructose isomerization also occurs in glucose pyrolysis and the decomposition
249 pathway via fructose is competitive with the direct fragmentation of glucose.
250 Fragmentation of glucose (reaction c) gives erythrose and glycolaldehyde. Erythrose
251 was the major C4 sugar from glucose in early stage of pyrolysis at 220 °C, and then, the
252 C4 sugar composition gradually shifted towards an erythrulose-rich one with an
253 increase in the heating time. This is explainable by the isomerization from erythrose into
254 erythrulose. Since the erythrulose/erythrose ratios at 220 °C/60 min and 250 °C/10 and
255 20 min were greater than 1, erythrulose is suggested to be more stable. This greater
256 stability of erythrulose can be also explained by its more substituted carbonyl structure
257 which is similar to 1,3-dihydroxyacetone as mentioned above.

258 Contrary to this, erythrulose was only observed as a C4 sugar from fructose
259 (Fig. 6), and the yield was as high as 30.8 wt% at 220 °C/30 min. This would be
260 explained by formation of a 3-hexulose via isomerization of fructose (reaction b),
261 although isolation of this C5 sugar failed probably due to its high decomposition
262 reactivity. A retro-aldol fragmentation of the 3-hexulose (reaction i) gave a C4 enol,
263 which was isomerized into more stable erythrulose preferably instead of erythrose.
264 Some of the erythrulose formed from glucose (220 and 250 °C) probably originated
265 from this reaction. Fragmentation into a C5 sugar (reaction m) is also possible for the
266 3-hexulose, although this sugar was not identified.

267 As for the formation of C3 sugars, many pathways (reactions e, g, j and o) are

268 possible as shown in Fig. 7. Interestingly, glyceraldehyde tends to form more selectively
269 than 1,3-dihydroxyacetone in the early stage of pyrolysis at 220 °C. In Fig. 7, only the
270 fructose fragmentation (reaction g) gives glyceraldehyde directly, while the initial
271 product of other reactions is a C3 enol, which can be isomerized into both
272 glyceraldehyde and 1,3-dihydroxyacetone. Accordingly, the isomerization into
273 glyceraldehyde is probably favored kinetically. The 1,3-dihydroxyl structure in the C3
274 enol would be preferable in association with the ether oxygen of TEGDE. As the
275 heating time increased, glyceraldehyde was gradually converted into the more
276 thermodynamically favorable 1,3-dihydroxyacetone. The greater isomerization rate
277 observed for the pyrolysis of glyceraldehyde (Fig. 4) may be explained by its higher
278 solubility in TEGDE which promoted the isomerization before heating and during the
279 heating up process. Although glucose and fructose were soluble in TEGDE only at high
280 temperature, glyceraldehyde and 1,3-dihydroxyacetone were soluble even at room
281 temperature.

282 Along with the glyceraldehyde fragmentation (Fig. 7), fragmentation of some
283 C4-C6 sugars (reactions c, d, l and o) also gives glycolaldehyde. This yield from
284 glucose was dramatically increased by increasing the pyrolysis temperature from 220 to
285 250 °C. Total yield of the identified fragmentation products reached a 74.9 wt% at 10
286 min. Direct fragmentation of glucose and subsequent fragmentation of erythrose
287 (reactions c and d, respectively) are expected to be the major sources of this enhanced
288 formation of glycolaldehyde. Such fragmentation reactions from aldoses may become
289 kinetically more favorable at higher temperature than the isomerization into fructose
290 and erythrulose which is thermochemically favorable.

291 Based on these lines of evidence, fragmentation via a cyclic six-membered
292 transition state involving a $\text{-OH}\cdots\text{O}=\text{C}<$ type of hydrogen bonding is suggested as a
293 selective fragmentation mechanism. Isomerization into the more stable ketose with a
294 more substituted $>\text{C}=\text{O}$ structure changes the fragmentation pathway. These reactions

295 are controlled both kinetically and thermodynamically.

296

297 3.3. Role of polyether

298 Fig. 8 shows the influence of the TEGDE loading level on the yields of the
299 fragmentation and isomerization products ($N_2/250\text{ }^\circ\text{C}/30\text{ min}$). With an increase in the
300 TEGDE/glucose ratio (T/G, w/w), the yield of glycolaldehyde increased drastically,
301 while the C4 sugars and glucose were observed only at the lower T/G ratios < 200 . The
302 yield of 1,3-dihydroxyacetone was almost constant in the T/G range 50-500.
303 Accordingly, the fragmentation reactivity tended to increase with an increase in the
304 loading level of TEGDE.

305 Fig. 9 illustrates the change in the IR spectrum (OH stretching region) of
306 1,3-dihydroxyacetone as the loading level of TEGDE (T/D, w/w) increased from 20 to
307 1000. 1,3-Dihydroxyacetone is known to exist as dimers in the solid phase [25], which
308 is formed through intermolecular hemiketalization. The broad IR spectrum at T/D 20
309 was similar to that reported for the solid sample [25]. The signals observed in the range
310 of $3100\text{-}3400\text{ cm}^{-1}$ were reduced by increasing the T/D ratio, and the spectrum (T/D
311 1000) became rather close to that [26] of the gaseous 1,3-dihydroxyacetone (monomer).
312 These results indicate that TEGDE assists the liberation of 1,3-dihydroxyacetone from
313 the dimer through cleavage of the hemiketal linkage. Hydrogen bonding between the
314 ether oxygens of TEGDE and the hemiketal/hemiacetal hydroxyl groups may act as a
315 base catalysis for conversion of hemiketal/hemiacetal into ketone/aldehyde and alcohol.
316 Similar conversion would be possible also for other C2-C4 compounds.

317 These IR results also suggest that a similar base-catalyzed reaction accelerates
318 the formation of the open-chain form of glucose from its pyranose and furanose isomers,
319 although a similar IR measurement was not possible for glucose due to the limited
320 solubility in TEGDE at ambient temperature. Recovery of glucose only at a low
321 TEGDE/glucose ratio of 20 (Fig. 8) is understandable with this proposal.

322 **Table 1** summarizes the yields of fragmentation and isomerization products
323 from glucose in TEGDE and three other polyethers, 18-crown-6, isosorbide
324 dimethylether (IDE) and diethyleneglycol dibutylether (DEGDBE) (N₂/250 °C/30 min).
325 TEGDE, 18-crown-6, and IDE exhibited similar product compositions, and the yield of
326 glycolaldehyde increased in the order: 18-crown-6 < TEGDE < IDE. This order may be
327 related to the ability of the ether oxygens to interact with the hydroxyl groups of glucose
328 as discussed above. The results of DEGDBE support this proposal, since DEGDBE with
329 only three oxygen atoms was not effective for these fragmentation reactions. Thus, the
330 selective fragmentation reaction occurs only when enough ether oxygen is provided by
331 the polyether.

332 Sulfolane, which is also an aprotic solvent, has been used for conversion of
333 cellulose into levoglucosan and other low MW products [27]. Unlike polyether, however,
334 formation of the dehydration products and colored substances is reported in sulfolane.
335 Sulfolane may accelerate the dehydration reaction with some specific mechanism.
336 Amarasekara et al. proposed the dehydration mechanism of fructose to
337 5-hydroxymethylfurfural in dimethyl sulfoxide [28].

338

339 3.4. Role of inter- and intramolecular hydrogen bonding in sugar pyrolysis: an
340 activation mechanism

341 Thermal glycosylation (**oligosaccharide** and anhydrosugar formation) and
342 dehydration reactions were effectively inhibited during pyrolysis of reducing sugars in
343 polyether. This can be explained by the formation of hydrogen bonds between the ether
344 oxygens and protons of the hydroxyl groups in the sugar. As illustrated in **Fig. 10** (for
345 glucose), all of the protons of the hydroxyl groups in glucose are expected to associate
346 with the ether oxygens when enough of the ether oxygen is provided. Under these
347 conditions, all of the hydroxyl oxygen atoms of glucose increase their electron densities,
348 and hence, the C₁-OH bond is expected to be stabilized for cleavage even in the

349 presence of the electron-donation from the lone pair of the ring oxygen. Consequently,
350 formation of the reactive intermediate (an oxonium ion) is inhibited.

351 Such discussion implies the role of intra and intermolecular hydrogen bonding
352 in the pyrolysis of reducing sugar melt where these hydrogen bonds are possible. Unlike
353 the polyether conditions, proton donation by hydroxyl groups of another glucose
354 molecule is also possible as illustrated in Fig. 10 (neat pyrolysis). Such proton donation
355 on the C₁-oxygen may act as an acid catalysis which promotes the elimination of OH
356 from the C₁ atom. In this process, the hydroxyl group which associates with the
357 C₁-oxygen is converted into the hydroxide anion. These transformations make the
358 glycosylation reaction quite easy.

359 Proposed dehydration mechanisms are illustrated in Fig. 11. The basicity of the
360 carbonyl oxygen is stronger than those of the ether oxygens. Consequently, the
361 -OH...O=C< type hydrogen bonding is possible even in polyether. This would be the
362 reason for the retro-aldol-type fragmentation selectively occurring in polyether.
363 Enolation is also expected because the aldose-ketose isomerization was observed in
364 polyether. Dehydration via an enol may be an important dehydration pathway of a
365 reducing sugar since simple polyalcohols such as glucitol were stable under the
366 conditions where dehydration of the reducing sugar was observed. This dehydration
367 reaction may be inhibited by the formation of hydrogen bonds between the ether
368 oxygens and the protons of the hydroxyl groups in the sugar. The hydroxyl group
369 hydrogen-bonded with the ether oxygen is stabilized for cleavage of the C-OH bond.
370 Contrary to this, the combination of the hydrogen bonds as illustrated in Fig. 11 (neat
371 pyrolysis) substantially enhances the dehydration reaction. This type of dehydration
372 mechanism may be involved in the pyrolysis of reducing sugar melt.

373

374

375 **4. Conclusions**

376 Reducing sugar was stabilized in polyether against glycosylation and other
377 dehydration reactions at 150-250°C. Reducing sugars were selectively converted into
378 the fragmentation products formaldehyde, glycolaldehyde, glyceraldehyde,
379 1,3-dihydroxyacetone, erythrose, and erythrulose. Formation of these products was
380 explained with a retro-aldol-type fragmentation mechanism including a cyclic
381 six-membered transition state. A conversion mechanism in polyether was proposed in
382 which the ether oxygen acts as a base to attract protons from the hydroxyl groups of the
383 sugar. The increasing electron densities of the oxygen atoms of the hydroxyl groups
384 may reduce the elimination reactivity of OH from sugar. Contrary to this, formation of
385 the cyclic six-membered $\text{-OH}\cdots\text{O}=\text{C}<$ type hydrogen bonding is possible even in
386 polyether since the carbonyl oxygen is more basic than the ether oxygen, which
387 promotes the retro-aldol-type fragmentation. As an alternative, an activation
388 (acid-catalysis) mechanism by proton-donation through intra and intermolecular
389 hydrogen bonding was proposed for glycosylation and dehydration mechanisms of the
390 neat pyrolysis of the melt sugar.

391

392

393 **Acknowledgments**

394 This work was supported by the Kyoto University Global COE program of “Energy
395 Science in the Age of Global Warming” and a Grant-in-Aid for Scientific Research (B)
396 (2) (No.20380103 2008.4-2011.3).

397

398 **References**

- 399 [1] R. C. Brown, *Biorenewable Resources: Engineering New Products from Agriculture*,
400 Wiley-Blackwell, Hoboken, 2003; pp. 3.
- 401 [2] M. S. Rana, V. Sámano, J. Ancheyta, J. Diaz, *Fuel* 86 (2007) 1216.
- 402 [3] S. Ahmed, A. Aitani, F. Rahman, A. Al-Dawood, F. Al-Muhaish, *Appl. Catal. A: Gen.*
403 359 (2009) 1.
- 404 [4] P. A. M. Claassen, J. B. van Lier, A. M. Lopez Contreras, E. W. J. van Niel, L.
405 Sijtsma, A. J. M. Stams, S. S. de Vries, R. A. Weusthuis, *Appl. Microbiol. Biotechnol.*
406 52 (1999) 741.
- 407 [5] A. V. Bridgwater, *J. Anal. Appl. Pyrol.* 51 (1999) 3.
- 408 [6] D. Mohan, C. U. Pittman, P. H. Steele, *Energy & Fuels* 20 (2006) 848.
- 409 [7] S. Rapagnà, N. Jand, P. U. Foscolo, *Int. J. Hydrogen Energy* 23 (1998) 551.
- 410 [8] P. Tomasik, P. Mieczysław, W. Stainsław, in: *Advances in Carbohydrate Chemistry*
411 *and Biochemistry*; R. S. Tipson, D. Horton (Eds.), Academic Press, New York, 1989, pp.
412 203-278.
- 413 [9] E. B. Sanders, A. I. Goldsmith, J. I. Seeman, *J. Anal. Appl. Pyrol.* 66 (2003) 29.
- 414 [10] T. L. Lowary, G. N. Richards, *Carbohydr. Res.* 198 (1990) 79.
- 415 [11] F. Shafizadeh, *J. Polym. Sci.: Polym. Symp.* 36 (1971) 21.
- 416 [12] Y. Houminer, S. Patai, *Israel J. Chem.* 7 (1969) 535.
- 417 [13] F. Shafizadeh, *J. Anal. Appl. Pyrol.* 3 (1982) 283.
- 418 [14] M. J. Antal, *Adv. Solar Energy* 1 (1983) 61.
- 419 [15] P. Tomasik, P. Mieczysław, W. Stainsław, in: *Advances in Carbohydrate Chemistry*
420 *and Biochemistry*; R. S. Tipson, D. Horton (Eds.), Academic Press, New York, 1989, pp.
421 279-335.
- 422 [16] K. Kato, *Agr. Biol. Chem.* 31 (1967) 657.
- 423 [17] Y. Houminer, S. Patai, *Israel J. Chem.* 7 (1969) 513.
- 424 [18] T. Hosoya, H. Kawamoto, S. Saka, *J. Anal. Appl. Pyrol.* 83 (2008) 64.

- 425 [19] T. Hosoya, H. Kawamoto, S. Saka, *Carbohydr. Res.* 341 (2006) 2293.
- 426 [20] T. Hosoya, H. Kawamoto, S. Saka, *J. Anal. Appl. Pyrol.* 77 (2006) 121.
- 427 [21] H. Sugisawa, H. Edo, *J. Food Sci.* 31 (1966) 561.
- 428 [22] S. Matsuoka, H. Kawamoto, S. Saka, *Carbohydr. Res.* 346 (2011) 272.
- 429 [23] G. G. Smith, B. L. Yates, *J. Org. Chem.* 30 (1965) 2067.
- 430 [24] B. L. Yates, J. Quijano, *J. Org. Chem.* 34 (1969) 2506.
- 431 [25] Y. Kobayashi, T. Igarashi, H. Takahashi, K. Higasi, *J. Mol. Struct.* 35 (1976) 85.
- 432 [26] R. Signorell, D. Luckhaus, *J. Phys. Chem. A* 106 (2002) 4855.
- 433 [27] H. Kawamoto, W. Hatanaka, S. Saka, *J. Anal. Appl. Pyrol.* 70 (2003) 303.
- 434 [28] A. S. Amarasekara, L. D. Williams, C. C. Ebede, *Carbohydr. Res.* 343 (2008) 3021.

Legends of Figures and Table

Fig. 1. Photographs of the pyrolyzates (a) and temperature dependence (b) of the recovery of glucose in the presence or absence of TEGDE (N₂/30 min). (●) neat glucose, (○) in TEGDE, TEGDE: tetraethyleneglycol dimethylether.

Fig. 2. GPC Chromatograms of glucose pyrolysis products in presence or absence of TEGDE (N₂/30 min), detector: RI (solid line) and UV_{254nm} (dotted line), Hex: cellohexaose, Tri: cellotriose, Glc: glucose, LG: levoglucosan, GA: glycolaldehyde, DHA: 1,3-dihydroxyacetone, TEGDE: tetraethyleneglycol dimethylether.

Fig. 3. Gas chromatograms of glucose pyrolysis products (N₂/220 °C/30 min). (a) neat glucose (TMS derivative), (b) neat glucose (oxime-TMS derivative), (c) in TEGDE (TMS derivative), (d) in TEGDE (oxime-TMS derivative), LG: levoglucosan, AF: 1,6-anhydro-β-D-glucofuranose, (●) glucose, (□) glycolaldehyde, (▲) glyceraldehydes, (△) 1,3-dihydroxyacetone, (◆) erythrose, (◇) erythrulose, TEGDE: tetraethyleneglycol dimethylether.

Fig. 4. Fragmentation and isomerization product formation from pyrolysis of 1,3-dihydroxyacetone and glyceraldehyde in TEGDE (20 mg/2 g) under N₂ at 250 °C. (▲) glyceraldehydes, (△) 1,3-dihydroxyacetone, (■) glycolaldehyde, (□) formaldehyde, TEGDE: tetraethyleneglycol dimethylether.

Fig. 5. Isomerization and retro-aldol fragmentation reaction of glyceraldehyde.

Fig. 6. Fragmentation and isomerization product formation from pyrolysis of glucose (a) and fructose (b) in TEGDE (20 mg/2 g) under N₂ at 220 and 250 °C. dotted line: total yield of fragmentation and isomerization product which were identified, (●) glucose, (○) fructose, (◆) erythrose, (◇) erythrulose, (▲) glyceraldehydes, (△) 1,3-dihydroxyacetone, (■) glycolaldehyde, TEGDE: tetraethyleneglycol dimethylether.

Fig. 7. Proposed isomerization and fragmentation pathways of glucose and fructose. FA: formaldehyde, GA: glycolaldehyde, GRA: glyceraldehydes, DHA: 1,3-dihydroxyacetone.

Fig. 8. Influence of TEGDE load on formation of fragmentation and isomerization products from glucose in TEGDE (N₂/250 °C/30 min). (●) glucose, (◆) erythrose, (◇) erythrulose, (▲) glyceraldehydes, (△) 1,3-dihydroxyacetone, (■) glycolaldehyde, TEGDE: tetraethyleneglycol dimethylether.

Fig. 9. Change in the IR spectra of 1,3-dihydroxyacetone dissolved in TEGDE; T/D: ratio of 1,3-dihydroxyacetone / TEGDE (w/w); TEGDE: tetraethyleneglycol dimethylether.

Fig. 10. A proposed mechanism explaining the stabilization of the reducing sugar against thermal glycosylation in

polyether.

Fig. 11. A proposed inhibition mechanism for dehydration occurring during pyrolysis of a reducing sugar in polyether.

Table 1 Yields of fragmentation and isomerization products obtained from pyrolysis of glucose in various polyether solvents (polyether/glucose = 20/1, w/w/ N₂/250 °C/30 min).

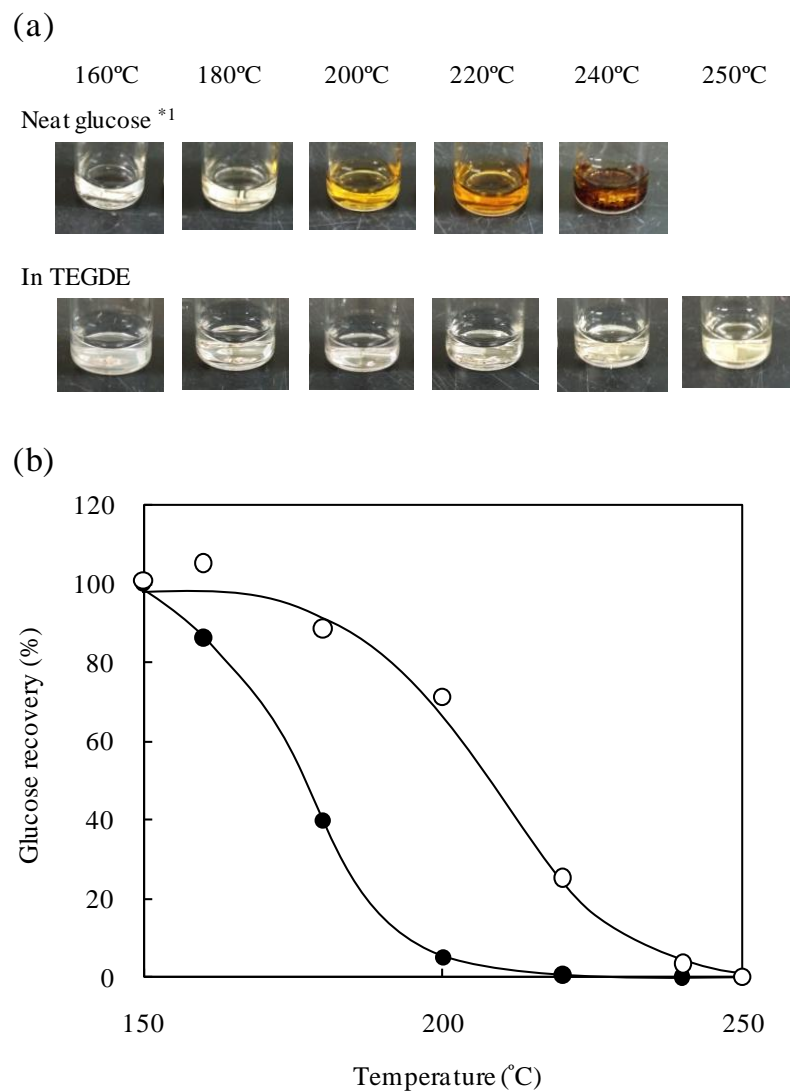


Fig. 1. Photographs of the pyrolyzates (a) and temperature dependence (b) of the recovery of glucose in the presence or absence of TEGDE ($N_2/30$ min). (●) neat glucose, (○) in TEGDE, TEGDE: tetraethyleneglycol dimethylether. *1: solubilized in water (1 mL) after pyrolysis.

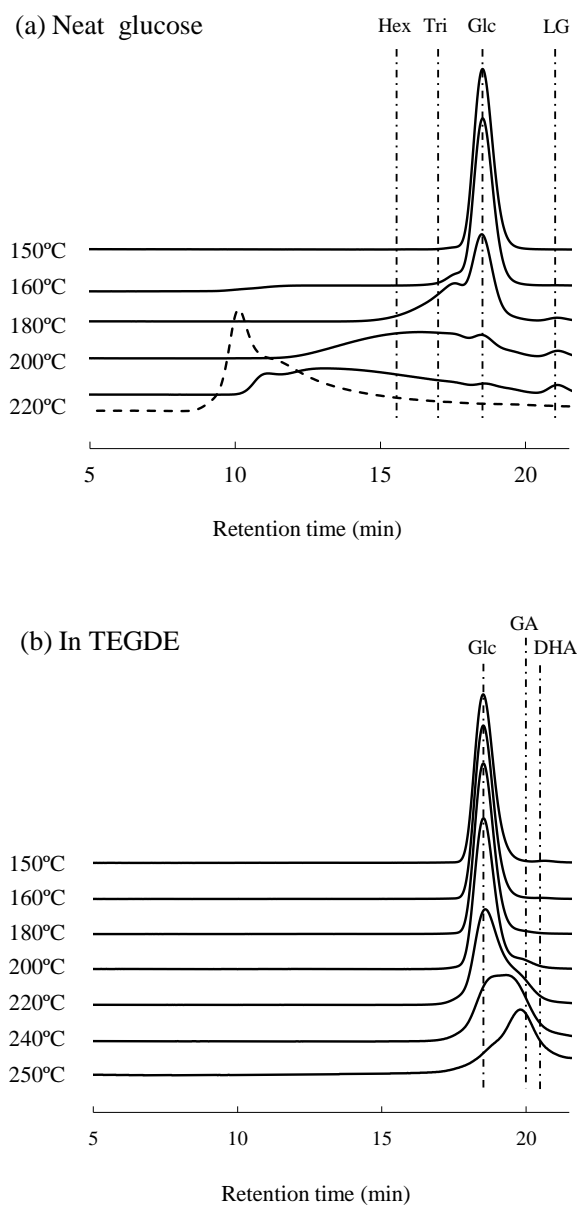


Fig. 2. GPC Chromatograms of glucose pyrolysis products in presence or absence of TEGDE ($N_2/30$ min), detector: RI (solid line) and UV_{254nm} (dotted line), Hex: cellohexaose, Tri: cellotriase, Glc: glucose, LG: levoglucosan, GA: glycolaldehyde, DHA: 1,3-dihydroxyacetone, TEGDE: tetraethyleneglycol dimethylether.

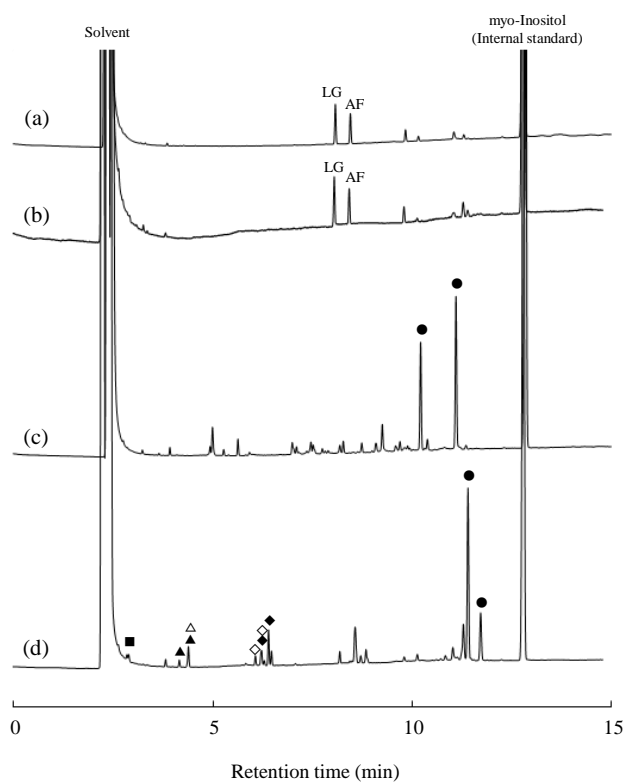


Fig. 3. Gas chromatograms of glucose pyrolysis products ($N_2/220\text{ }^\circ\text{C}/30\text{ min}$). (a) neat glucose (TMS derivative), (b) neat glucose (oxime-TMS derivative), (c) in TEGDE (TMS derivative), (d) in TEGDE (oxime-TMS derivative), LG: levoglucosan, AF: 1,6-anhydro- β -D-glucofuranose, (●) glucose, (□) glycolaldehyde, (▲) glyceraldehydes, (△) 1,3-dihydroxyacetone, (◆) erythrose, (◇) erythrulose, TEGDE: tetraethyleneglycol dimethylether.

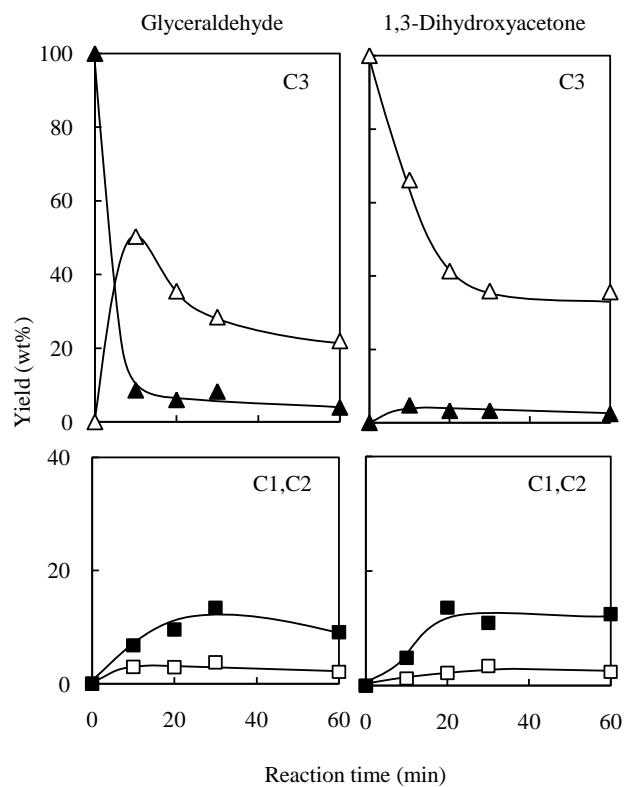


Fig. 4. Fragmentation and isomerization product formation from pyrolysis of 1,3-dihydroxyacetone and glycerolaldehyde in TEGDE (20 mg/2 g) under N₂ at 250 °C. (▲) glycerolaldehydes, (△) 1,3-dihydroxyacetone, (■) glycolaldehyde, (□) formaldehyde, TEGDE: tetraethyleneglycol dimethylether.

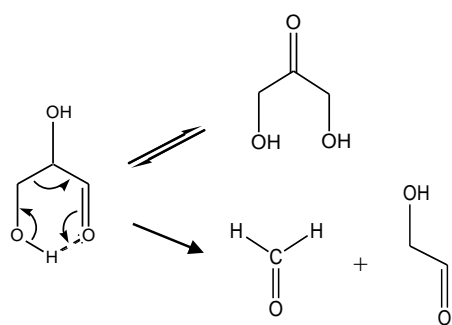


Fig. 5. Isomerization and retro-aldol fragmentation reaction of glyceraldehyde.

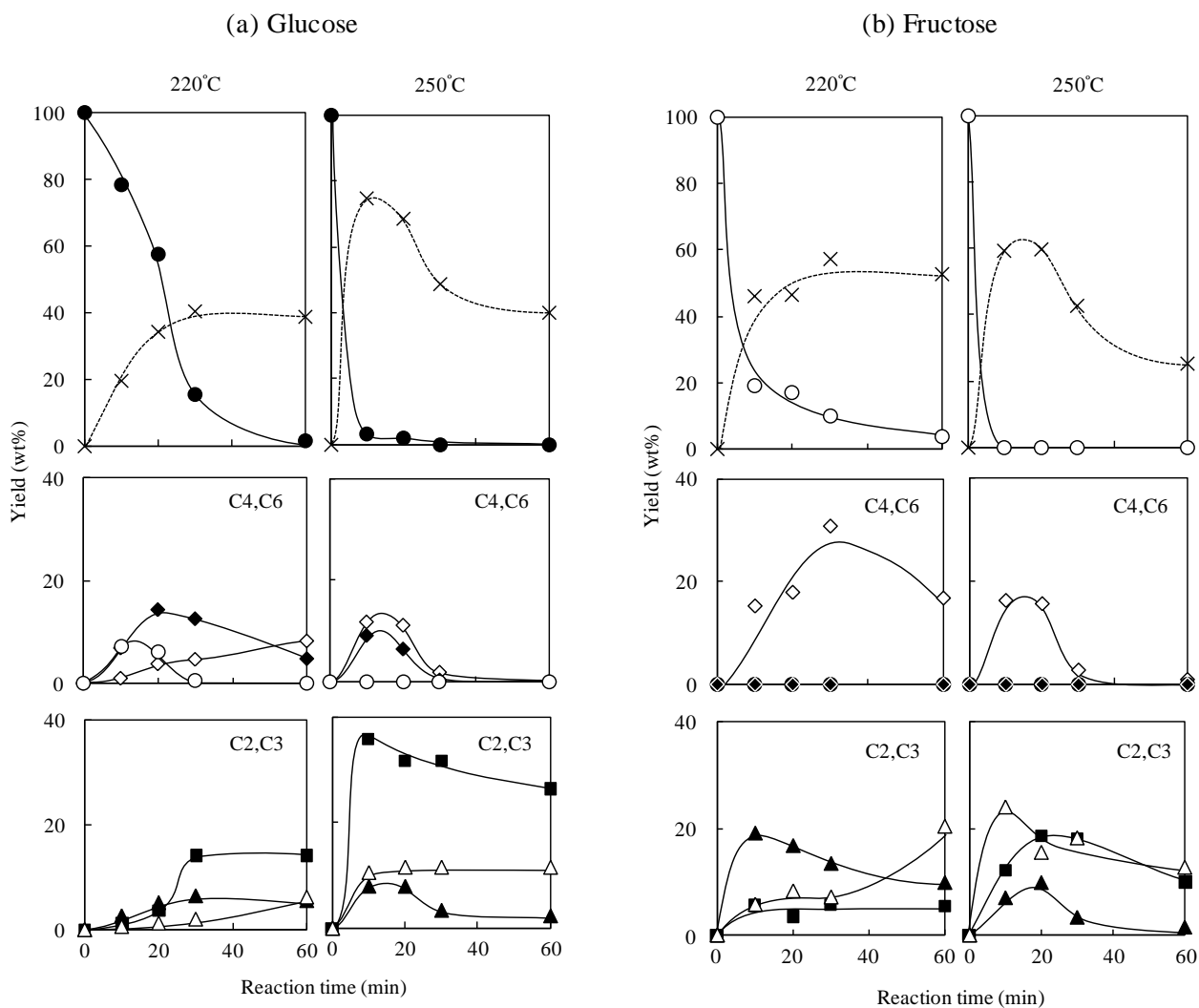


Fig. 6. Fragmentation and isomerization product formation from pyrolysis of glucose (a) and fructose (b) in TEGDE (20 mg/2 g) under N_2 at 220 and 250 °C. dotted line: total yield of fragmentation and isomerization product which were identified, (●) glucose, (○) fructose, (◆) erythrose, (◇) erythrulose, (▲) glyceraldehydes, (△) 1,3-dihydroxyacetone, (■) glycolaldehyde, TEGDE: tetraethyleneglycol dimethylether.

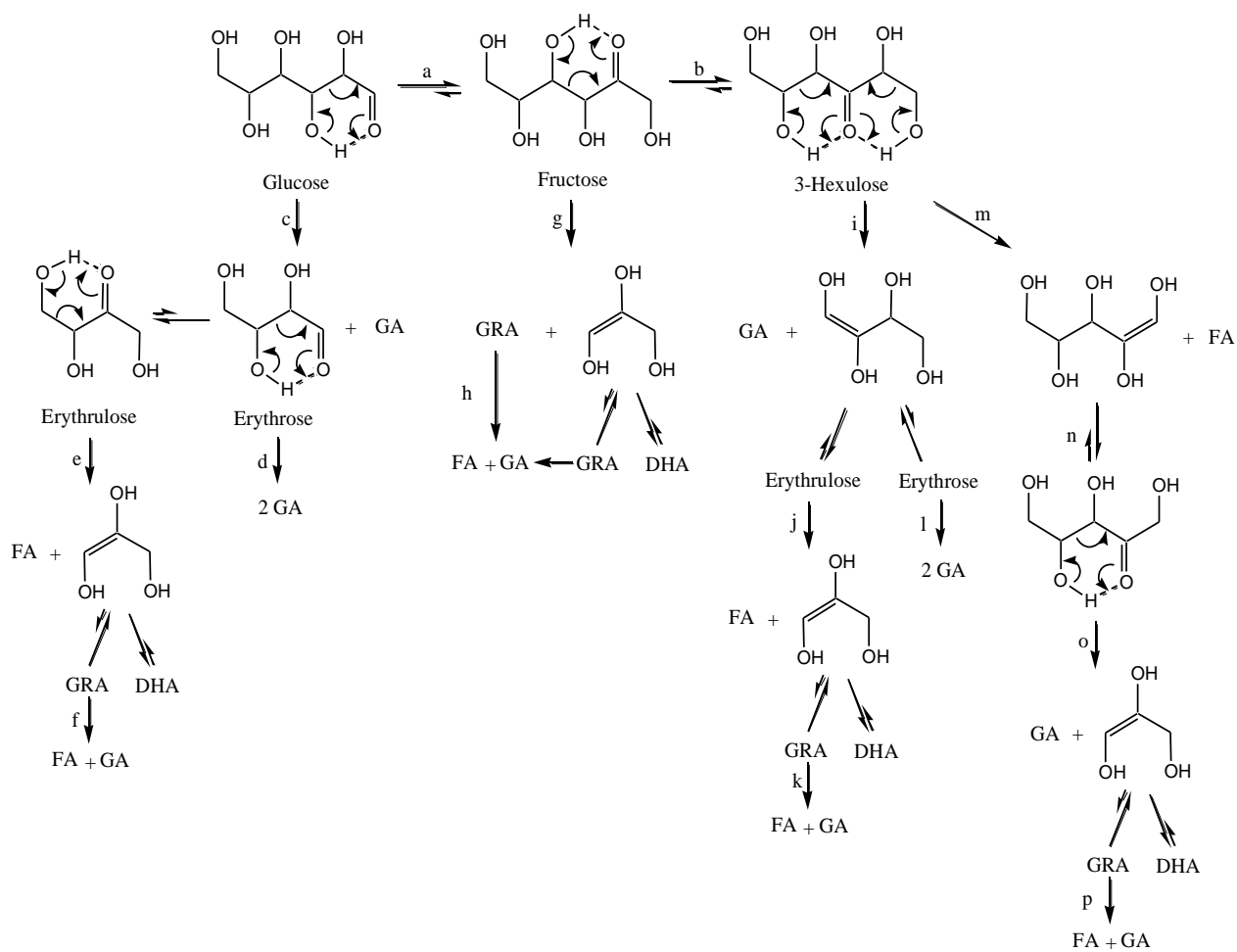


Fig. 7. Proposed isomerization and fragmentation pathways of glucose and fructose. FA: formaldehyde, GA: glycolaldehyde, GRA: glyceraldehydes, DHA: 1,3-dihydroxyacetone.

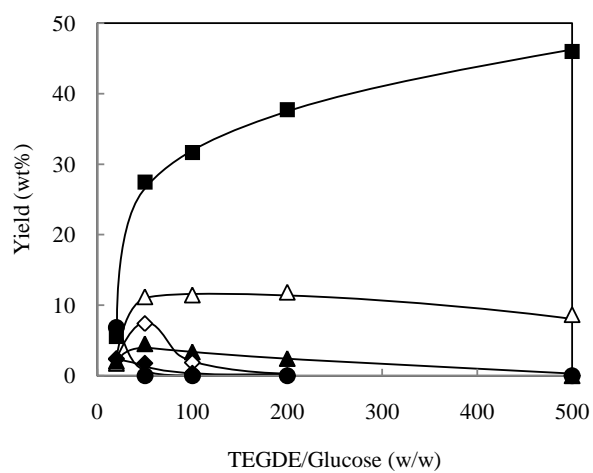


Fig. 8. Influence of TEGDE load on formation of fragmentation and isomerization products from glucose in TEGDE ($N_2/250\text{ }^\circ C/30\text{ min}$). (●) glucose, (◆) erythrose, (◇) erythrulose, (▲) glyceraldehydes, (△) 1,3-dihydroxyacetone, (■) glycolaldehyde, TEGDE: tetraethyleneglycol dimethylether.

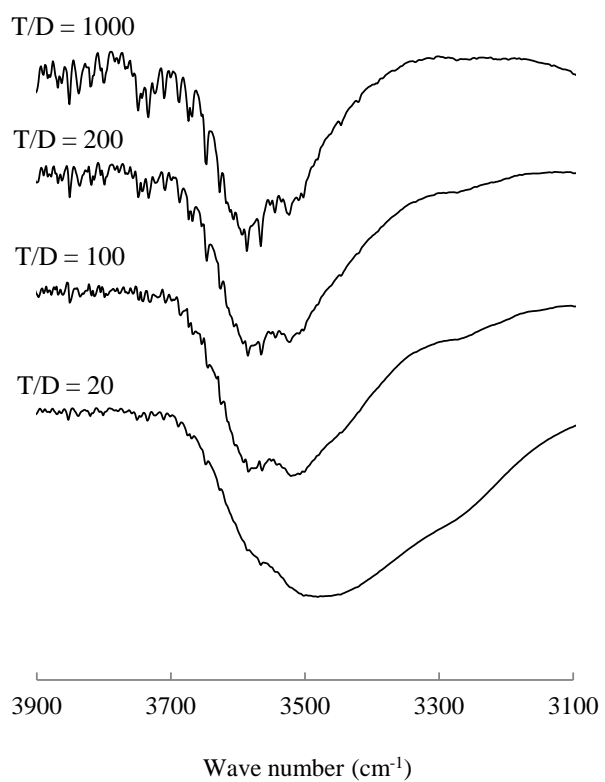
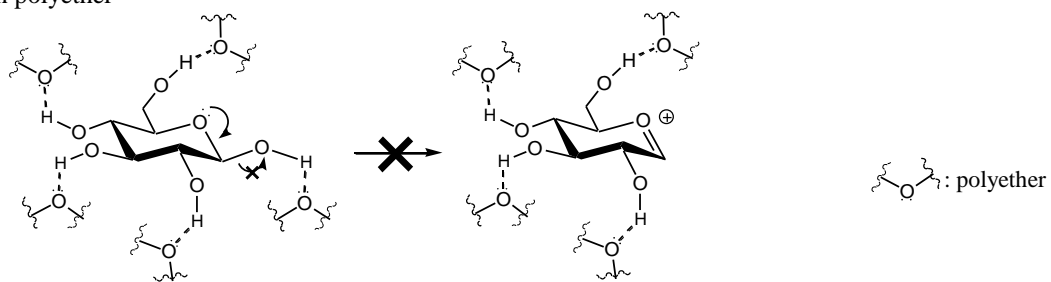


Fig. 9. Change in the IR spectra of 1,3-dihydroxyacetone dissolved in TEGDE; T/D: ratio of 1,3-dihydroxyacetone / TEGDE (w/w); TEGDE: tetraethyleneglycol dimethylether.

In polyether



Neat pyrolysis

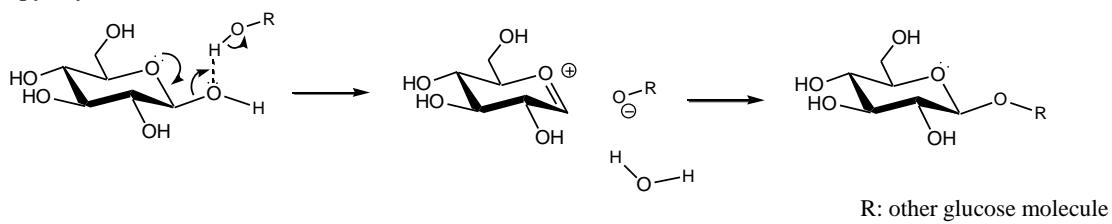
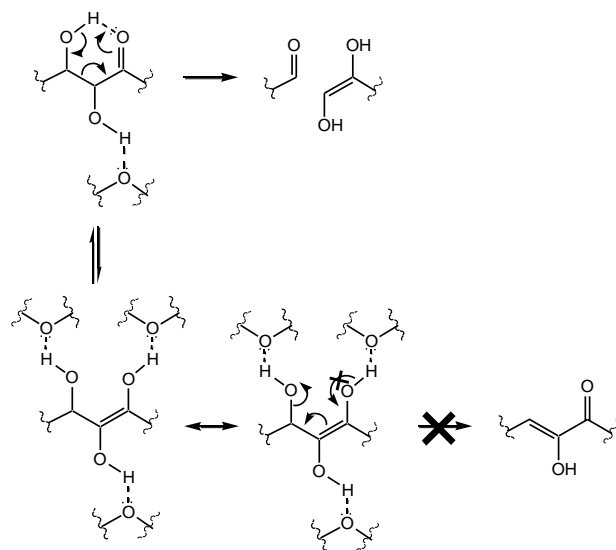


Fig. 10. A proposed mechanism explaining the stabilization of the reducing sugar against thermal glycosylation in polyether.

In polyether



Neat pyrolysis

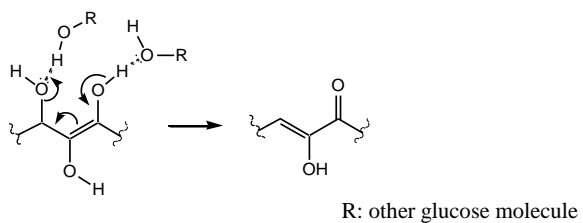
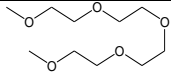
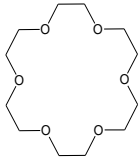
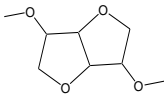
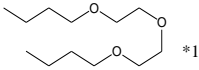


Fig. 11. A proposed inhibition mechanism for dehydration occurring during pyrolysis of a reducing sugar in polyether.

Table 1 Yields of fragmentation and isomerization products obtained from pyrolysis of glucose in various polyether solvents (polyether/glucose = 20/1, w/w/ N₂/250 °C/30 min).

Solvent	Yield (wt%)						Glucose recovery (%)
	GA	GRA	DHA	ETR	ETRL	Fru	
 TEGDE	40.6	7.4	12.4	0	2.8	0	0
 18-crown-6	35.1	5.9	17.2	0	5.4	0	0
 IDE	56.0	2.2	10.8	0	5.0	0	0
 DEGDBE	4.1	1.3	1.1	2.4	1.6	1.27	16.5

*1 Glucose was not completely dissolved, GA: glycolaldehyde, GRA: glyceraldehydes, DHA: 1,3-dihydroxyacetone, ETR: erythrose, ETRL: erythrulose, Fru: fructose, TEGDE: tetraethyleneglycol dimethylether, IDE: isosorbide dimethylether, DEGDBE: diethyleneglycol dibutylether.